

## Fibre-like structure formation in fava bean protein based extrudates: effects of extrusion inputs and potential of outputs for process control

Clara Barnés-Calle, Grau Matas, Pere Gou\*, Elena Fulladosa

IRTA (Institute of Agrifood Research and Technology). Food Quality and Technology. Finca Camps i Armet, s/n, 17121 Monells, Girona, Spain

### ARTICLE INFO

**Keywords:**

Extrusion outputs  
Torque  
Anisotropy index  
Texturisation  
Fava bean protein concentrate  
Fibre-like structure  
Control

### ABSTRACT

High moisture extrusion processing (HMEP) is a complex process in which product formulation and extrusion conditions play a key role in fibre-like structure formation. The aim of this work was to study the effect of process input parameters (formulation, liquid feed, and extrusion temperature) on the texture development of a high moisture extrudate (HME) based on fava bean protein concentrate (FBPC), combined with a different protein source (pea protein isolate - PPI) or an oil ingredient (extra virgin olive oil (EVOO)). The influence of extrusion outputs (melt temperature, pressure, and torque) on texture parameters and its potential to control the texturisation process was also investigated. Formulation (protein source and added oil) and moisture content had a significant effect on textural characteristics of HME, while a variation of barrel temperature of 10 °C (from 145 to 155 °C) was not sufficient to influence the final product texture. Addition of PPI to FBPC-based HME increased hardness and fibrousness of the product, while oil addition had a lubricating effect which difficulted the formation of fibre-like structures in the direction of the extrusion flow. Out of the studied extrusion outputs, torque was highly correlated with the HME textural characteristics, showing potential for inline control of the HMEP process.

### 1. Introduction

One of the biggest challenges in the elaboration of plant-based meat alternative products is to mimic animal muscle texture. High-moisture extrusion processing (HMEP) is being studied as an approach to achieve this challenge. During HMEP, the application of high temperature, pressure, and shear cause proteins to unfold, aggregate, and realign (Samard et al., 2019), forming fibrous structures along the direction of the extrusion flow. However, HMEP is a complex process in which product formulation and extrusion conditions play a key role in fibre-like structure formation. Numerous recent works have been published regarding the effect of HMEP inputs (e.g., water feed, screw speed or extrusion temperature) on HME texture development using different protein sourced formulations. Several authors have shown that increased moisture content softens the texture of HME from different protein sources such as soy protein isolate (Zang et al., 2025), yellow pea and fava bean protein isolates and concentrates (Ferawati et al., 2021), and yeast protein isolates (Xia et al., 2023). Moreover, various works have shown that extrusion temperatures can improve HME texturization. For example, Sun et al. (2023) showed that higher extrusion

temperatures allowed better fiber formation in HME from pea protein isolate. Screw speed has also been identified to influence HME texture. However, its effect seems to depend on the moisture content. For instance, Ferawati et al. (2021) reported that increased screw speed led to an increased degree of texturisation in HME from pea and fava bean at higher moisture contents (69–70 %) but showed no clear relationship with HME texture at lower moisture contents (<68 %).

Furthermore, HME from pea and fava bean protein sources – both protein isolates and concentrates – have shown promising potential as non-allergenic alternatives to substitute the widely used soy protein source, successfully allowing the formation of fibrous structures by HMEP in previous studies (Ferawati et al., 2021; Toldrà et al., 2025; Barnés-Calle et al., 2024). However, to our knowledge, there are no works published blending both protein sources to produce HME. In this regard, further studies integrating pea and fava bean proteins could provide insights into the possibility of combining diverse protein ingredients, whose functional characteristics may be influenced by the protein source, as well as the extraction and drying methods used in their obtention (Chandran et al., 2024).

Moreover, the addition of other ingredients – such as oils and fats – to

\* Corresponding author.

E-mail address: [pere.gou@irta.cat](mailto:pere.gou@irta.cat) (P. Gou).

protein-based HME is raising interest, as it can contribute to improve the juiciness and taste in plant-based meat analogue formulations (Saavedra Isusi et al., 2023) and to better mimic the nutritional profile of animal products. However, its use during HMEP may negatively affect texture development (Zhang, Zhao, et al., 2023). Nevertheless, Wang et al. (2022) developed an improved oil addition approach that consisted in adding oil-in-water (O/W) emulsion during HMEP. This enhanced texture attributes such as chewiness, making them similar to those of cooked chicken breast, still allowing fibre formation.

Despite the advances achieved until now and the different hypotheses that have risen to explain protein texturisation through HMEP (van der Sman and van der Goot, 2023), today it still mostly remains a trial-and-error matter which requires evaluation of the impact of extrusion parameters on the texture of the final high moisture extrudates (HME) mostly using adapted conventional physicochemical methods (Schreuders, Schlangen, et al., 2021). Since protein texturisation is related to the anisotropic character of the HME, it can be instrumentally assessed by relating textural properties such as tensile strength (Saldanha do Carmo et al., 2021) or cutting strength (Wittekk, Karbstein, et al., 2021) in two different dimensions of the product (e.g., parallel and perpendicular to the extrusion flow). Furthermore, alternative approaches such as the evaluation of texture through visual images of the final product, have revealed multi-layered phase systems deformed in the direction of the extrusion flow that show a "V-shape" or elliptical pattern that is more pronounced in highly texturised HME (Osen, 2017; Wittekk, Karbstein, et al., 2021). Besides, non-invasive methods based on spectrometric analysis (Yao, Liu, and Hsieh, 2004) or imaging techniques (Ranasinghesagara et al., 2005) that enable rapid non-invasive characterisation of the final HME texture and could be useful for the control of the HMEP are being studied. In this regard, the extruder responses (outputs) such as motor torque, die pressure, and specific mechanical energy (SME) can also reflect the characteristics of the final HME (Osen et al., 2014). Extrusion outputs (namely SME and maximum product temperature) have been demonstrated to be useful for process control and optimization of whey protein microparticulation (Wolz and Kulozik, 2017), and have also been recently investigated in combination with calorimetric measurements for high moisture texturisation prediction of soy and pea protein (Högg and Rauh, 2023). However, further investigation on extrusion outputs alone and its potential use to control texture development of different protein sources could be valuable to bring the actual trial-and-error perspective closer to a real-time control of the process. Given the considerations outlined above, the hypotheses of the research were as follows: (i) pea and fava bean protein blends allow fibre formation by HMEP, (ii) oil-in-water addition during HMEP have minimal effect on HME texture; (iii) extrusion outputs can be used to control protein texturization.

Therefore, the aim of this work was to investigate how process inputs, such as liquid feed and extrusion temperature, impact the texture development of a HME based on fava bean protein concentrate (FBPC) when combined with complementary ingredients such as a different protein source (pea protein isolate (PPI)) or an oil ingredient (extra virgin olive oil (EVOO)) in emulsion with water. The study also examined the influence of extrusion outputs—pressure, torque and melt temperature at the die—on HME texture in order to explore its potential to control the texturisation process.

## 2. Materials and methods

### 2.1. Materials, formulations and reference sample preparation

All HME samples were elaborated using fava bean protein concentrate (FBPC) with a 60.4 % of protein and 3.7 % of fat on dry basis, and 6.9 % of moisture content (FFBP-60-D, AGT Food and Ingredients, Minot, ND, USA), in addition to bottled water (Font Vella, Aguas Danone SA, Spain). Different formulations were achieved by adding EVOO (Gourmet, Vilamalla, Spain) and PPI containing 87.8 % of protein and

9.7 % of fat on dry basis, and 7.0 % moisture (PISANET™ M9, Cosucra, Belgium). The formulations included one recipe with 100 % of FBPC and three other elaborated adding different ingredients in the liquid or the solid fractions at different concentrations, as specified in Table 1. As PPI showed good texturisation properties on its own in previous studies (Barnés-Calle et al., 2024), it was added to FBPC in a 20 % and 50 % proportion as a complementary ingredient to evaluate its combined effect. Composition of the solid fraction (included in Table 1) was calculated for each formulation based on the moisture, protein and fat content of FBPC and PPI.

On the other hand, a 4 % of EVOO was added in emulsion with the water in the liquid fraction, prepared according to Wang et al. (2022) using 2 % of PPI to stabilize the emulsion. EVOO was added at 4 % to obtain HME with similar fat content to cooked chicken breast (3.6 % fat approx., according to USDA (2019)), which was considered as the reference meat product in the present study. Cooked chicken breasts were used as reference samples and were prepared according to Chiang et al. (2019), with some modifications (Barnés-Calle et al., 2024). Three chicken breasts were packed individually in plastic bags (HT3000 Barrier Bag®, Sealed Air, Charlotte, NC, USA) and cooked in a heated water bath set at 77 °C until their internal temperature reached 75 °C. Chicken exudate was eliminated, and chicken reference samples were cooled down at room temperature (22 °C ± 2 °C) for at least 1 h.

### 2.2. Experimental design and HME sample elaboration

FBPC-based HME samples were elaborated using a laboratory-scale co-rotating and intermeshing twin-screw extruder (Process 11, Thermo Fisher Scientific Inc., Waltham, MA, USA) with a 40 screw length to diameter ratio (L/D). Fig. 1 shows the different screw elements that were used: feed screw elements (FS), mixing elements oriented at 0° from the axis (ME-0), mixing elements oriented at 90° from the axis (ME-90) and discharge elements (EXT). Screw configuration consisted of an initial conveying zone formed by 15 FS, followed by two mixing areas (ME-0/ME-90/ME-0/ME-0/ME-0/ME-0/ME-0/ME-90/ME-0/ME-0/ME-90/ME-0; generating different angles of 30°, 60° and 90° degrees between them) separated by a 8-FS conveying zone, and a final conveying zone formed by 10 FS and a closing EXT.

Along the barrel, the extruder had a feeding zone (Z1), 7 temperature zones (Z2-Z8) and an additional heating zone at the die (Fig. 1), and was equipped with a peristaltic pump (Reglo ICC Pump, ISMATEC, IDEX Health and Science LLC, Oak Harbor, WA, USA) and a vertical volumetric feeder with agitator (MiniTwin, Brabender Technology GmbH, Duisburg, Germany) to feed the liquid and the solid fractions, respectively, into the extruder at different rates. Calibration of the volumetric feeder was carried out independently for each of the solid fraction formulations, as its dosing speed may vary based on the nature of the raw input materials. A cooling die (internal dimensions: H 4 mm x W 19 mm x L 125 mm) supplied by a refrigerated bath circulator ("KISS K6", HUBER, Peter Huber Kältemaschinenbau AG, Offenburg, Germany) set at 20 °C was assembled at the end of the extruder outlet.

During the extrusion process, screw speed was set at 650 rpm and

	Liquid Fraction (LF)			Solid Fraction (SF)			Calculated composition of SF	
	Water	EVOO	PPI*	FBPC	PPI	Moisture (%)	Protein (% db)	Fat (% db)
F1	100	0	0	100	0	6.9	60.4	3.7
F2	100	0	0	80	20	6.9	65.9	4.9
F3	100	0	0	50	50	7.0	74.1	6.7
F4	94	4	2	100	0	6.9	60.4	3.7

EVOO: extra virgin olive oil; PPI: pea protein isolate; FBPC: fava bean protein concentrate.

\* PPI content used to stabilize emulsion in LF; db: dry basis.

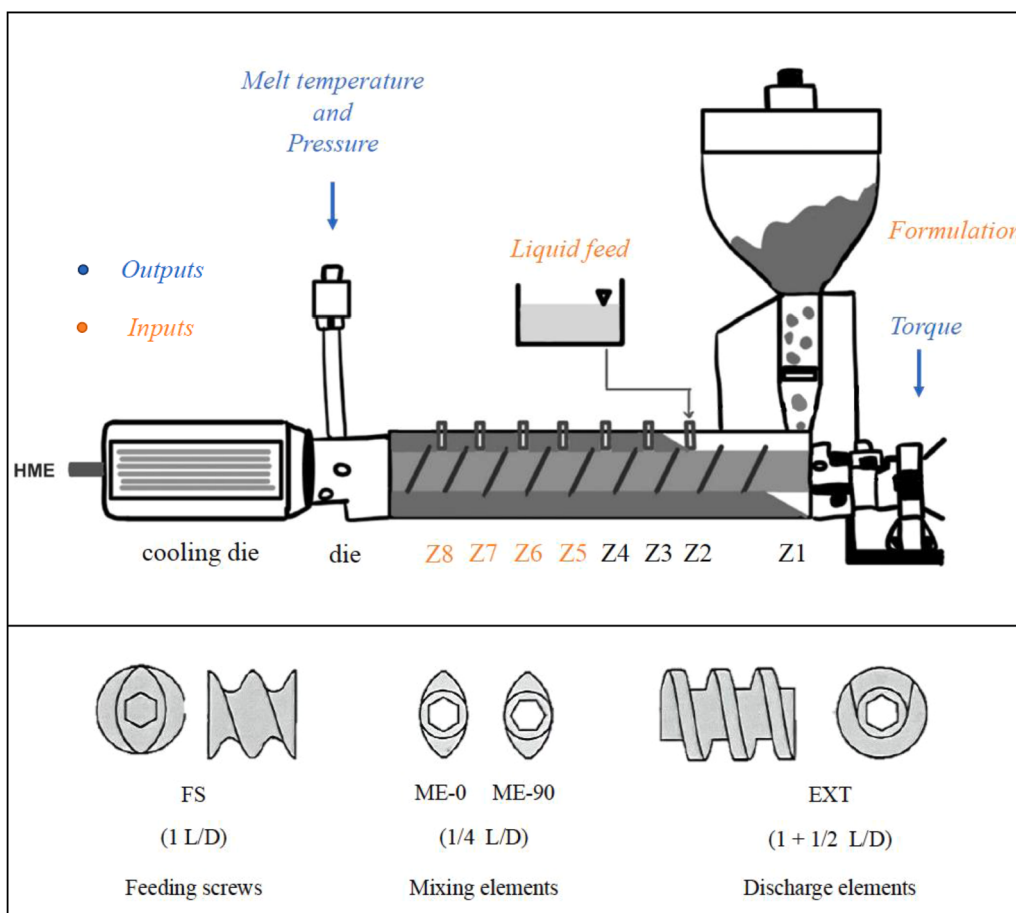


**Fig. 1.** Schematic view of the extruder with the feeding zone (Z1) and temperature zones (Z2-Z8), die zone and cooling die and representation of screw elements and their respective length to diameter ratio (L/D). FS: feeding screws, ME-0: mixing elements oriented at 0° from the axis, ME-90: mixing elements oriented at 90° from the axis, EXT: discharge elements. Extrusion input parameters are indicated in orange and output measurement points in blue. Source adapted from “High moisture extrusion of pea protein isolate to mimic chicken texture: Instrumental and sensory insights”, by Barnés-Calle et al. 2024, *Food Hydrocolloids*, 154, 110,129, p 2 (<https://doi.org/10.1016/j.foodhyd.2024.110129>).

temperatures in heating zones Z2 to Z4 were fixed at 50, 90 and 110 °C, and the die zone at 100 °C, as described in a previous work (Barnés-Calle et al., 2024). The global (liquid + solid fractions) feeding rate was set constant at approximately  $12 \pm 0.2$  g/min.

Using the four formulations based on FBPC (Table 1), HME were elaborated at different extrusion conditions modifying liquid feed (50 or 60 %) and barrel temperature in heating zones Z5 to Z8 (145 or 155 °C), according to the experimental design.

Experimental ranges were defined based on preliminary results, combining different extrusion conditions (liquid feed and extruder barrel temperatures) at which HME from FBPC could be elaborated continuously without collapsing the extruder (either because of too much or too little water or temperature). A total of 16 experiments were obtained at different conditions combining the three extrusion inputs (formulation, liquid feed, and barrel temperature) (see experimental design in Table 2).

Once the defined experimental conditions were stable, samples were collected in triplicates (at intervals of 10 min between each replicate), sealed in plastic bags, and stored at  $-18 \pm 2$  °C until further analysis.

### 2.3. Extrusion outputs

During the elaboration process of HME samples, three outputs were recorded: melt temperature ( °C) and pressure (bar) at the die (the last stage at the extruder barrel before the cooling of the product) using an ensembled inline probe (H DTA 1133-1/2-100-93-PC-T-J, Thermo

Fisher Scientific Inc., Waltham, MA, USA) and torque (expressed in %), which represents the work necessary to turn the twin screws and transport the product through the extruder in relation to the maximum that can be achieved (6 N.m), measured and displayed by the extruder software (see Fig. 1). Moreover, SME is a scale-independent measure of the mechanical energy applied to the material being extruded (Kantrong et al., 2018) that can be useful to establish a relationship between the processing variables and the properties of extrudates and to characterize the process (Cotacallapa-Sucapuca et al., 2021). It can be calculated using the mass flow rate, the screw speed, and the torque (Godavarti and Karwe, 1997; Guerrero et al., 2012). However, as mass flow rate and screw speed were set constant in the present study, torque was directly used instead of the SME.

### 2.4. Physicochemical analysis

#### 2.4.1. Moisture content

HME samples were thawed at  $4 \pm 1$  °C, 24 h before analysis. Once thawed, they were brought to room temperature ( $20 \pm 2$  °C). Moisture content of HME samples was determined according to the official gravimetric method (AOAC 1990). Approximately 5 g of sample was weighed, cut into small pieces, and dried at  $103 \pm 2$  °C until constant weight was reached. All analyses were performed in duplicate.

#### 2.4.2. Instrumental texture analysis

For texture analysis, HME samples were cut into  $19 \times 19$  mm pieces

**Table 2**

Range of extrusion outputs and mean and standard deviation of measured moisture content of HME samples, for each formulation and extrusion process ( $n = 3$ ).

Formulation	Inputs		Outputs			Measured moisture content (%)
	Liquid feed (%)	T (°C)	Torque (%)	T Melt (°C)	P (bar)	
F1	60	145	5.3 ± 0.6 <sup>fg</sup>	89.0 ± 0.0 <sup>ef</sup>	6.0 ± 0.0 <sup>f</sup>	63.83 ± 0.383 <sup>a</sup>
F1	60	155	6.0 ± 0.0 <sup>fg</sup>	91.0 ± 0.0 <sup>bcd</sup>	2.3 ± 0.6 <sup>e</sup>	64.02 ± 0.190 <sup>a</sup>
F1	50	145	8.0 ± 1 <sup>cd</sup>	91.0 ± 0.0 <sup>bcd</sup>	11.0 ± 0.0 <sup>b</sup>	53.95 ± 0.592 <sup>c</sup>
F1	50	155	10.0 ± 0.0 <sup>a</sup>	91.3 ± 0.6 <sup>bcd</sup>	12.7 ± 1.5 <sup>ab</sup>	50.60 ± 0.962 <sup>de</sup>
F2	60	145	5.3 ± 0.6 <sup>g</sup>	91.3 ± 0.6 <sup>bcd</sup>	4.7 ± 1.15 <sup>de</sup>	62.58 ± 0.062 <sup>a</sup>
F2	60	155	6.0 ± 1.7 <sup>g</sup>	91.7 ± 2.3 <sup>a</sup>	4.3 ± 2.3 <sup>e</sup>	62.60 ± 0.202 <sup>a</sup>
F2	50	145	9.3 ± 1.2 <sup>ab</sup>	91.7 ± 0.6 <sup>abc</sup>	12.7 ± 2.3 <sup>a</sup>	51.56 ± 0.435 <sup>d</sup>
F2	50	155	9.3 ± 1.2 <sup>a</sup>	91.7 ± 0.6 <sup>abc</sup>	13.0 ± 1.7 <sup>a</sup>	49.68 ± 0.496 <sup>e</sup>
F3	60	145	5.7 ± 0.6 <sup>fg</sup>	91.3 ± 0.6 <sup>bcd</sup>	5.3 ± 1.15 <sup>cd</sup>	63.55 ± 0.211 <sup>a</sup>
F3	60	155	Unstable process			
F3	50	145	8.0 ± 1.7 <sup>de</sup>	90.3 ± 1.5 <sup>de</sup>	8.7 ± 2.3 <sup>c</sup>	55.25 ± 0.053 <sup>c</sup>
F3	50	155	8.3 ± 1.5 <sup>cde</sup>	90.7 ± 1.2 <sup>cde</sup>	8.7 ± 2.3 <sup>c</sup>	55.34 ± 0.229 <sup>c</sup>
F4	60	145	6.7 ± 0.6 <sup>def</sup>	88.3 ± 0.6 <sup>f</sup>	6.7 ± 0.6 <sup>c</sup>	57.25 ± 0.753 <sup>b</sup>
F4	60	155	5.0 ± 0.0 <sup>g</sup>	91.0 ± 0.0 <sup>bcd</sup>	3.3 ± 0.6 <sup>e</sup>	58.43 ± 0.858 <sup>b</sup>
F4	50	145	8.3 ± 0.6 <sup>bc</sup>	90.0 ± 0.0 <sup>de</sup>	11.0 ± 0.0 <sup>b</sup>	47.76 ± 0.383 <sup>f</sup>
F4	50	155	8.0 ± 0.0 <sup>cd</sup>	90.7 ± 0.6 <sup>bcd</sup>	7.3 ± 0.6 <sup>c</sup>	45.78 ± 0.075 <sup>g</sup>

<sup>a-g</sup> Different letters within a same column indicate significant differences between samples ( $p < 0.05$ ). T: barrel temperature; F1: FBPC; F2: FBPC + 20 % PPI; F3: FBPC + 50 % PPI; F4: FBPC + EVOO; FBPC: fava bean protein concentrate; PPI: pea protein isolate; EVOO: extra virgin olive oil.

maintaining their original thickness of 4.5 mm. Chicken reference samples were sliced at  $4.5 \pm 0.5$  mm with a slicer machine (GP 350 EUROCORT AYERBE, Navarra, Spain) and cut manually into  $19 \times 19$  mm pieces to reproduce the size of the HME samples. Shear test analysis were performed with a texture analyser (TA.HDPlus, Stable Micro Systems, Surrey, UK) using a 5 kg cell load and a Warner-Bratzler blade set with a rectangular slot blade at a probe speed of 2 mm/s. Shear test was performed in both transversal and longitudinal orientation to the extrusion flow or chicken meat fibres (Fig. 2), and the corresponding maximum shear forces were recorded ( $F_T$  and  $F_L$ , respectively, expressed

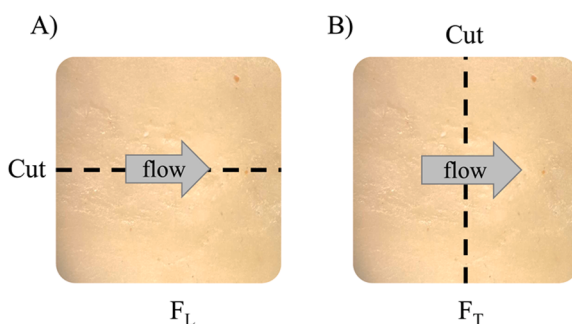


Fig. 2. Representation of shear cuts applied longitudinally (A) and transversally (B) to the extrusion flow or fibre direction, to measure longitudinal ( $F_L$ ) and transversal ( $F_T$ ) shear force.

in N). Six measurements per sample and per test orientation were performed and averaged. Data were acquired and treated using the 6.1.16.0 version of Exponent Stable Micro Systems software (Stable Micro Systems Ltd., UK).

The anisotropy index (AI) was also used as a texturisation indicator and was calculated by the ratio between  $F_T$  and  $F_L$  according to Wittek, Karbstein, et al. (2021):

$$AI = F_T/F_L$$

AI values close to 1 indicate uniform texture with low material anisotropy (Osen et al., 2014), whereas AI values  $>1$  indicate anisotropy which can be explained by fibre-like structure formation in the direction of the extrusion flow.

## 2.5. Macro- and microstructure of HME

### 2.5.1. Visual evaluation of HME texturisation

For the visual evaluation of texturisation, V-shape and elliptical profile (also known as parabolic pattern) were assessed (Högg and Rauh, 2023). HME samples were manually folded along their longitudinal axis (parallel to the extrusion flow, as represented in Fig. 3A) to visualise the V-shape. HME layers were also manually separated by carefully pulling the samples apart from the extremes of their longitudinal axis, revealing the elliptical profile (Fig. 3B). Pictures of the longitudinal fold and the elliptical profile of HME samples were taken using a binocular stereozoom microscope (SZM-1, OPTIKA Microscopes, Ponteranica, BG, Italy) with 7x magnification and a phone camera with 12 MP resolution (iPhone SE 2020, Apple Inc., Cupertino, CA, United States).

### 2.5.2. Confocal scanning laser microscopy

A highly texturised HME sample was selected to be studied at a microstructural level. The selected sample was fixed in Bacto-agar (Sigma Aldrich, Merck Group, MO, USA) 8 % (in distilled water) and cut in slices of 100  $\mu$ m with a vibratome (VT1000S, Leica Biosystems, IL, USA). These were then stained using Rhodamine B (0.1 mg/ml) and were observed using a confocal laser scanning microscope (FV1000, Olympus, Tokyo, Japan) equipped with a UPLSAPO 10x/0.4 objective and a 561 nm diode laser.

### 2.5.3. Scanning electron microscopy

The selected highly texturised HME samples were manually cut in approximately 1 cm x 1 cm pieces. They were fixed with 2.5 % glutaraldehyde, 2 % paraformaldehyde in PB 0.1 M for 2 h at 4 °C, post-fixed with 1 % osmium tetroxide with 0.8 % potassium ferrocyanide for 2 h and dehydrated in increasing concentrations of ethanol (50, 70, 90, 96, 100 %). Samples were then chemically dried with hexamethyldisilazane (HMDS) and sputtered-coated with a thin layer of PdAu for 4 min at 20 mA (Emitech K550X sputter coater). Once fixed and dried, HME samples were imaged using a SEM Hitachi S570 (Hitachi Ltd., Tokyo) operating at 20 kV.

## 2.6. Statistical analysis

Linear regression using the standard least squares method was applied to model the effect of extrusion inputs and outputs on HME texture using JMP 16 software (JMP Statistical Discovery LLC, NC, USA).

To study the effect of process inputs on HME texture, linear models were fitted including formulation and extrusion temperature as main effects, the moisture content as a covariate and the double interactions between the main effects and the covariate. The non-significant effects and interactions ( $p > 0.05$ ) were dropped from the linear models. All mean values were compared by Tukey test. Correlation between the different outputs was evaluated using a Pearson correlation matrix.

To study the effect of extrusion outputs on HME texture, multiple regression models were fitted for each formulation including as independent variables melt temperature, torque and pressure. Due to

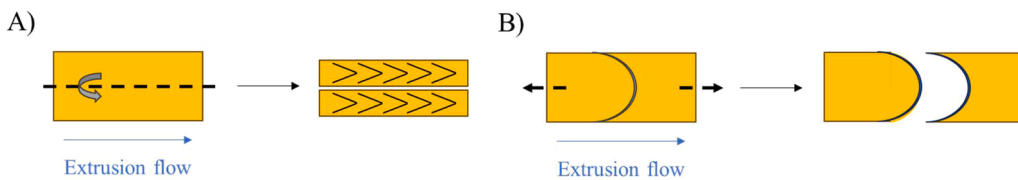


**Fig. 3.** Schematic view of the preparation procedure for the visual evaluation of the V-shape (A) and the elliptical profile (B) of a HME sample.

collinearity between torque and pressure ( $r = 0.91$ ,  $p < 0.001$ ), evaluated using Pearson correlation, and the non-significant effect of melt temperature, simple regression models were fitted for each formulation including only torque as independent variable.

### 3. Results and discussion

#### 3.1. Characterisation of HMEP

Extrusion outputs and moisture content of the elaborated HME obtained when using different formulations and extrusion conditions are presented in [Table 2](#). In general, higher values of torque and pressure were reached at lower liquid feed rate (50%). This can be related to the increasing melt viscosity (resistance to flow) with decreasing moisture content ([Akdogan, 1996](#)). At lower moisture contents, the extrusion melt circulated less fluidly through the barrel (higher viscosity), causing a greater resistance to rotation of the screws. This resulted in higher torque and pressure at the die, which are known to be highly sensible to the conditions in the solid feeding zone of the extruder (Z2) ([Mennig, 1987](#)) and to melt viscosity at the die ([Abeykoon et al., 2009](#)), respectively. In contrast, melt temperature presented minor variations across different extrusion conditions and formulations. This fact was attributed to the small differences between extrusion barrel temperature levels (10 °C of variation) and a decrease in temperature at the last stage of the heating process (die temperature was fixed at 100 °C for all experiments, as detailed in [Section 2.2](#)), which moderated the possible variations in melt temperature at the die. In this regard, it is worth mentioning that due to the decrease in temperature in the last stage of the barrel, the measured temperature did not necessarily correspond to the maximum temperature reached by the melt during the process. In fact, [Wittek, Karbstein, et al. \(2021\)](#) showed that melt temperatures of soy and wheat blends reached 133 °C when barrel temperatures were set between 155 and 165 °C using the same extruder and cooling die dimensions than in the present study. Moreover, although the use of a wider range of barrel temperatures would have probably shown a greater effect on melt temperature, the combination of higher temperatures at high moisture content (60%) would have compromised the obtention of continuous and consistent product, as reported by [Toldrà et al. \(2025\)](#). At the same time, this imposes a limitation on sample size due to the narrower extrusion conditions that can be explored, which is also a reality in the industrial-scale elaboration of HME. Still, taking all of this into consideration, a slight tendency of melt temperature to increase was still observed at higher extrusion temperatures.

It is important to highlight that during extrusion of F3 at high liquid feed (60%) and high temperature (155 °C), irregularities in the process were experienced. In general, increased PPI content in the formulation caused more variation in extrusion outputs compared to other formulations as shown in [Table 2](#). It could be hypothesised that these greater variations could be related to a combination of factors affecting protein functionality and structure, which may be influencing the melt behaviour. For example, extraction methods used to obtain the protein concentrates and isolates can have an impact on their functionality ([Chandran et al., 2024](#)), concentrates being usually obtained by milder methods, which better preserve protein characteristics ([Hopf et al., 2023](#)). In this regard, PPI functionality could potentially have been more affected by the extraction method used, influencing melt behaviour.

Moreover, [Ferawati et al. \(2021\)](#) found that pea protein denaturation temperature of pea protein (88–89 °C) was lower than that of fava bean (95–97 °C), which can also cause different behaviour of the ingredient during HMEP. In addition, for F3, variability was even greater at higher liquid feed (60%) and higher barrel temperature (155 °C) causing larger variations and reaching a higher melt temperature in comparison to other formulations. This supposed a larger temperature drop when the matrix entered the cooling die and caused undesired flashing of water to steam as the product left the die, unbalancing the system and causing oscillation of all output parameters. For this reason, the product obtained under these conditions was not homogeneous and the sample could not be considered representative. Therefore, characterization of this sample was not included to avoid distortions in the statistical analysis.

#### 3.2. Moisture content of HME

Moisture content of HME varied from 45.8 % to 64.0 % ([Table 2](#)) and, as expected, it decreased with lower liquid feed for all formulations. Moreover, the addition of EVOO in the liquid fraction in F4, which partially substituted the added water, slightly reduced the final moisture content of the HME in comparison to the other formulations. However, although liquid feed was controlled, final moisture content of HME elaborated under the same conditions presented variations. This might be in part attributed to moisture content variations of the raw materials. These may originate during sample preparation or incurred through relative air humidity ([Wagner et al., 1987](#)) and could impact the quality and structuring of extrudates ([Tsagareishvili et al., 2019](#)). Besides, each dosing equipment may inherently experience some degree of deviation. In addition, despite the dosage of the volumetric feeder was calibrated for each of the formulations used, this dosage system is sensitive to material build-up, which may lead to some fluctuation of the mass flow output at constant screw speed ([Bekaert et al., 2022](#)). All of the mentioned causes may contribute to the variation in the real moisture content of HME and in their characteristics. Therefore, in order to account for it in the present study, the effect of measured moisture content of HME was evaluated instead of theoretical water feed.

#### 3.3. Effect of formulation, extrusion temperature and moisture content on HME texture

Liquid feed was not the only factor defining the final HME moisture content (as discussed in [Section 3.2](#)). Therefore, analysed moisture content was included as a covariate instead of liquid feed to build the

**Table 3**

Effect summary (p-value) of moisture content, formulation, extrusion temperature, and their double interactions on HME texture parameters ( $F_L$ ,  $F_T$ , and AI).

Source	$F_L$	$F_T$	AI
Moisture content	0.049*	<0.0001*	0.294
Formulation	<0.0001*	<0.0001*	0.018*
Temperature	0.772	0.643	0.707
Formulation*Moisture content	0.365	<0.0001*	<0.0001*
Temperature*Formulation	0.900	0.051	0.362
Temperature*Moisture content	0.895	0.598	0.791

\*  $p < 0.05$  indicates a significant effect.

linear models.

**Table 3** shows the effect summary of the main input effects (moisture content, formulation, Temperature, and all double interactions on HME texture parameters. Extrusion temperature and all double interactions containing this variable had no significant effect on HME texture within the range of temperatures studied (145–155 °C) ( $p > 0.05$ ). According to literature, temperature is an important factor for protein texturisation, and its increase can enhance structure unfolding (Soeda, 1994). However, each protein has an ideal processing temperature at which the highest quality texture is created (Plattner, 2020). In this regard, results on the effect of extrusion temperature on HME texture are not consistent across different published works. Recent studies have reported increased cutting force with a 10 °C increase in barrel temperature during HMEP using different raw materials including FBPC (Saldanha do Carmo et al., 2021) and PPI with oat protein blends (Immonen et al., 2021). Contrarily, Ribeiro et al. (2024), reported that higher temperatures resulted in softer soy HME, with increased visual and instrumental anisotropy. Moreover, Chen, Wei et al. (2010) found that extrusion temperature significantly influenced the tensile strength of HME from soy protein isolate, while it did not impact its hardness and chewiness, and showed no clear effect on the degree of texturization. These inconsistencies might be explained by the combined effect of extrusion temperature and additional factors such as moisture content (Zhao et al., 2023) and total flux (related with the residence time of the matrix inside the extruder barrel). In this regard, with the extrusion conditions established in the present study, a 10 °C increase from 145 °C to 155 °C in barrel temperature was not enough to produce detectable textural changes in the obtained HME.

In contrast, both formulation and moisture content had a significant effect on all texture parameters, and the interaction formulation\*moisture content was significant for  $F_T$  and AI, but not for  $F_L$ . In the cases where this interaction was significant, effect of moisture content was studied for each formulation separately. Fig. 4A shows the effect of moisture content on  $F_L$ . It can be observed that the effect of moisture content was the same for all formulations, obtaining higher values of  $F_L$  at lower moisture content, comprising values between 6.4 N and 20.0 N. Chicken reference samples, however, presented  $F_L$  values between 7.9 N and 8.6 N (presented in Fig. 4A), indicating that HME at lower moisture content were generally harder than real cooked chicken meat. As expected, a lower moisture content in the mixture caused the obtention of less fluid and more viscous matrices, which lead to harder final HME samples. Our results are in agreement with other works which reported that lower moisture content resulted in harder texture of HME using diverse protein sources including soy (Zang et al., 2025), yellow pea and fava bean (Ferawati et al., 2021), and yeast (Xia et al., 2023). This can be attributed to a higher relative protein concentration in the melt at lower moisture content, which enhances protein-protein cross-linking formation as described in other works (Singh et al., 2024).

Formulation also had a significant effect on  $F_L$  ( $p < 0.05$ ), which is shown by different letters in Fig. 4A. F3 presented a significantly higher  $F_L$  in comparison to the other formulations ( $p < 0.05$ ), meaning that increase in PPI in the formulation allowed the obtention of harder HME samples. This can be related to the higher protein content of PPI compared to FBPC, which increases the total protein content in F3 and the possibility of protein-protein cross-linking (Zhang, Liu, et al., 2018). Similar results were found by Kantanen et al. (2022), who reported that HME from fava bean protein isolate (FBPI) were harder than HME from FBPC and also attributed it to a higher protein content. Contrarily, Ferawati et al. (2021) obtained harder textures for HME prepared from FBPC than from FBPI. These differences between studies could be related to the composition of the raw materials. Protein-rich powders can have different composition, especially in the case of protein concentrates, where a high percentage of their composition is not protein. The non-protein fraction usually contains small percentages of water, fat, and carbohydrates. Carbohydrates have been described to influence HME texturisation by enhancing protein-polysaccharide interactions

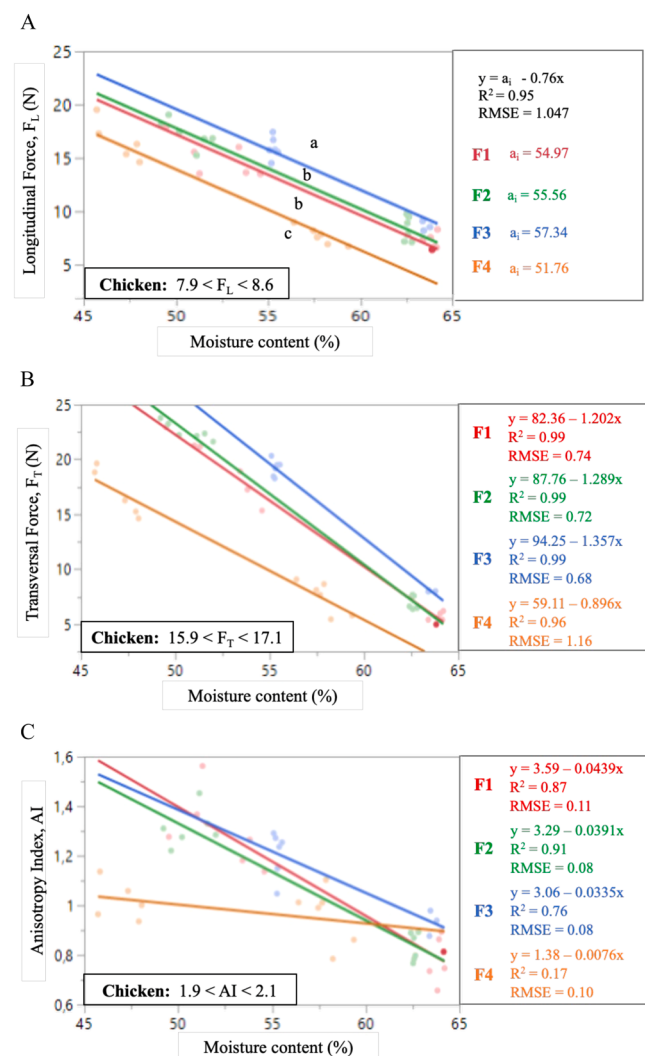


**Fig. 4.** Relationship between moisture content (%) and longitudinal force ( $F_L$ ; Fig. 4A), transversal force ( $F_T$ ; Fig. 4B) and anisotropy index (AI; Fig. 4C) for each formulation. Coloured lines show the linear regression for each formulation (F1 in red, F2 in green, F3 in blue and F4 in orange). Different letters indicate significant differences between formulations when the interaction moisture content\*formula was not significant.  $F_L$ ,  $F_T$ , and AI value range of chicken reference samples are included in Fig. 4A, 4B, and 4C, respectively.

over protein-protein interactions, affecting textural and rheological properties (Pietsch et al., 2019). Due to their hydrophilic character, these ingredients can enhance the interaction between proteins, water, and lipids upon extrusion and help create the fibrous texture, attracting water and controlling the aqueous phase rheology (Schmid et al., 2022). However, depending on their molecular size, carbohydrates can also act as effective plasticisers (Alee et al., 2021) and can reduce intermolecular interactions between molecular chains by attracting water molecules and destroying hydrogen bonds, increasing the plasticity of extrudates (Gao et al., 2019), which can challenge texturisation. More specifically, during HMEP, starch (present in FBPC) is converted from a natural particle state to a gelatinization state, and protein denaturation and rupture of starch particles during extrusion may result in additional interactions between the two types of polymers, which in turn can affect product characteristics (Hao et al., 2024). In this same work, it was reported that after extrusion treatment, protein formed a thin filamentous network that wrapped starch granules, connecting cracks present in the dough and forming a compact structure. This might cause HME to be denser, and therefore harder, if processed at adequate temperatures.

However, at the same time, starch granules can be severely damaged and degraded at extreme temperatures, decreasing the strength of the network structure (Hao et al., 2024; Ali et al., 2020).

Furthermore, as previously mentioned, the extraction methods used to obtain the protein concentrates and isolates can also have an impact on their functionality. Particularly complex methods such as wet extraction, which are often required to obtain high protein purity (e.g. protein isolates), cause protein denaturation and aggregation and have an impact on protein functionality (Hopf et al., 2023), which at the same time can affect the product hardness and cutting strength (Verfaillie et al., 2024). In addition, HME texture may also be influenced by other factors such as content of protein fractions – prolamins, globulins, albumins, and glutelins (Osborne, 1924) – of the source used, as they have different functional characteristics (Oluwajuyitan and Aluko, 2025). Therefore, despite protein content is one of the main aspects influencing HME texture, the use of different protein sources or protein sources extracted by different methods, is also relevant to be further considered regarding HME texture.

Moreover, the HME samples elaborated with F4 were significantly softer ( $p < 0.05$ ), indicating that although oil addition is interesting to obtain a more meat-like nutritional profile, it can compromise HME texture formation. This can be explained by the plasticizing effect of oil on macromolecules, which reduces the friction between them by increasing molecular mobility resulting in a decrease in viscosity (Ilo et al., 2000). In this context, the fat content of PPI could also influence the texture of HME. However, the higher protein content of PPI, compared to FBPC, is more significant in determining the texture than the fat content.

As in the case of  $F_L$ ,  $F_T$  increased at lower moisture contents (Fig. 4B), reaching values up to 23.8 N. In this case,  $F_T$  values obtained at low moisture contents were closer to chicken samples ( $F_T$  between 15.9 N and 17.1; presented in Fig. 4B) than in the case of  $F_L$  values. However, this effect was not the same in all the formulations (interaction formulation\*moisture content was significant;  $p < 0.05$ ). The increase of  $F_T$  at lower moisture contents was lower with formulation F4. Moreover, in general, HME elaborated with F3 presented higher transversal force, while F4 samples were the softest. In the case of  $F_T$ , this difference between formulations was more evident with decreasing moisture content. While the difference between F4 and the rest of formulations was of maximum 5 N at moisture contents above 60 %, this gap almost doubled at moisture contents below 55 %. As discussed before, lower moisture content, on one side, and increasing PPI content in the formulation, on the other, implied a higher relative protein content in the mixture. Thus, the encouragement of protein-protein cross-linking formation at lower moisture content, added to the increased possibility of these interactions in HME samples from F3 due to higher PPI content, enhanced the difference of transversal force between formulations.

In general, higher values were reached for  $F_T$  compared to the same longitudinal parameter. This can be related to how texturisation takes place. In HMEP, fibre-like structure formation occurs during the cooling stage, where the outer area of the matrix is cooled first (as it is in contact with the refrigerated surface), and the core is cooled the latest (as it is further away from the cooling die walls). This causes the internal region to be more fluid and advance at a higher speed than the external, developing velocity gradients and shear forces in the peripheral zones that allow the orientation and alignment of proteins and result in the formation of layers (Akdogan, 1999), deformed in the direction of the extrusion flow and adopting the elliptical shape of the flow profile (Wittek, Zeiler, et al., 2021). Greater friction in the cooling die produced by more viscous melts allows the formation of these layers, obtaining more textured HME. This causes the necessary force to cut across (transversal) and along (parallel) the extrusion flow to be different, thus indicating better texturisation at higher difference between the two cutting forces (Osen et al., 2014).

For the reasons mentioned above, higher values of AI (ratio  $F_T/F_L$ ) were achieved for HME with lower moisture content (Fig. 4C), reaching

values  $>1$  in samples produced using F1, F2, and F3, meaning that use of less water during HMEP using FBPC, and FBPC-PPI allowed the obtainment of more texturised HME. Viscous flow at lower moisture content caused greater shearing in the cooling die, encouraging the formation of anisotropic structures. At the same time, in line with the findings for longitudinal and transversal force, lower moisture content (higher relative protein content) enhanced cross-linking and favoured the formation of anisotropic structures as it allowed a major fraction of protein to be texturised. In fact, the HME from FBPC and FBPC-PPI blends produced presented higher anisotropy compared to the AI of a commercial soy-based HME (1.17), calculated from cutting force values reported by Elshamy et al. (2025). Still, maximum AI values obtained for HME samples were lower than AI of chicken samples (AI between 1.9 and 2.0; presented in Fig. 3C), indicating that despite enabling the formation of fibrous structures and even achieving better texturisation than commercial analogues, HMEP of FBPC and FBPC-PPI blends alone could still not completely mimic chicken texture.

At high moisture contents ( $>60\%$ ), friction along the die was reduced and no fibrous character along the direction of extrusion flow was observed for any of the studied formulations through instrumental analysis ( $AI \leq 1$ ). Moreover, AI values of HME elaborated adding EVOO (F4) hardly exceeded 1 under any of the studied extrusion conditions. Oil lubricated the cooling die and reduced the shearing and friction of the melt against the walls, inhibiting the formation of anisotropic structures. In addition, the plasticizing effect of oil can cause the disruption of non-covalent protein-protein interactions (such as hydrogen bonds, van der Waals interactions, and electrostatic forces), according to the gel theory (Aiken et al., 1947). Additionally, it can mask these binding sites from each other, thereby preventing their re-aggregation (Opaluwa et al., 2024). Similarly, this effect has also been reported for leguminous protein-based extrusion before. Gwiazda et al. (1987) had previously reported that the addition of oil to soybean extrudates led to a loss of anisotropic structure formation, and Chen, Zhang, et al. (2022) showed that the presence of fatty acids inhibited aggregation of legumin and vicilin (also present in fava bean), causing a negative effect in the anisotropic structure formation of pea protein-based extrudates.

Overall, besides oil addition to the formulation – which clearly hindered texturisation – results showed that HME texturisation degree was more affected by moisture content than by the formulation used, as high AI were achieved for all F1, F2 and F3 at low moisture content, whilst no anisotropy was observed for any of the formulations at high moisture contents (as showed in Fig. 4).

### 3.4. Effect of extrusion outputs on HME texture

HMEP inputs, specifically moisture content (related to liquid feed rate) and the formulation used as discussed in Section 3.3, have an important effect on HME texture and can be useful for process design. However, control of texturisation would be particularly interesting to do inline, during product elaboration. The measured outputs (torque, melt temperature and pressure) during the process were evaluated with the premise that they could provide real-time useful information that would allow to make the necessary changes during HMEP to ensure well-texturised products saving time and resources, as an alternative to controlling moisture content of the final product. In the present study, melt temperature did not have a significant effect on any textural parameter (results not shown;  $p > 0.05$ ), and for this reason it was not included in the models. Besides, a high correlation between pressure and torque was observed ( $r = 0.91$ ,  $p < 0.001$ ), having torque less variation than pressure (see Table 2). Therefore, out of the three outputs only torque was examined as a potential parameter to control HME texturisation. Along with torque, effect of formulation and the interaction torque\*formulation were also assessed (Table 4).

Fig. 5 shows the relationship between torque and the texture parameters for each formulation (coloured lines). While torque and

**Table 4**

Effect summary (p-value) of torque, formulation, and the interaction torque\*formulation on HME texture parameters ( $F_L$ ,  $F_T$ , and AI).

Source	$F_L$	$F_T$	AI
Torque	<0.0001*	<0.0001*	<0.0001*
Formulation	0.003	<0.0001*	<0.0001*
Torque*Formulation	0.088	0.335	0.052

\*  $p < 0.05$  indicates a significant effect.

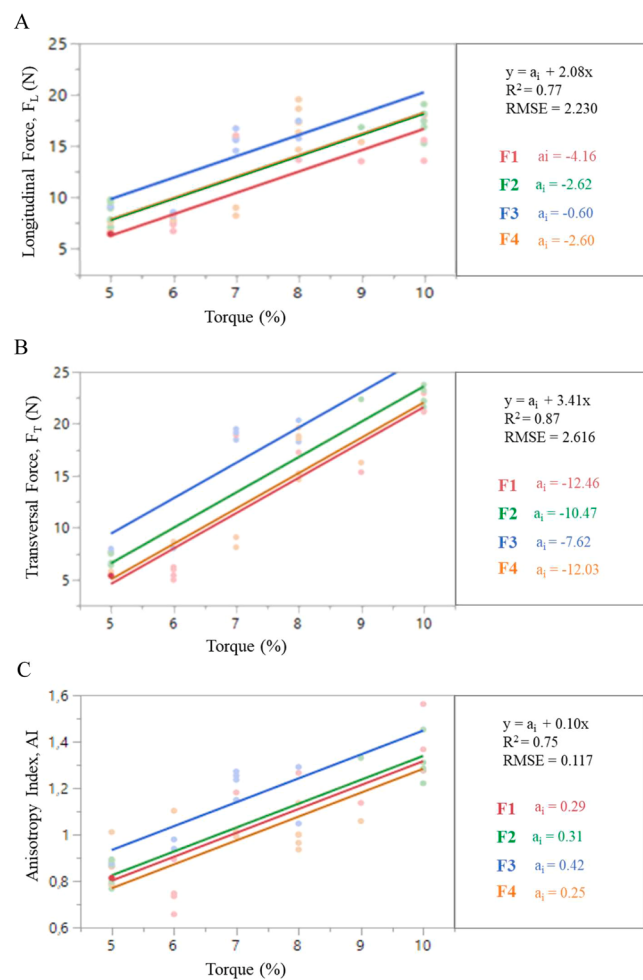


**Fig. 5.** Relationship between torque ( %) and longitudinal force (A), transversal force (B) and anisotropy index (C) for each formulation. Coloured lines show the linear regression for each formulation (F1 in red, F2 in green, F3 in blue and F4 in orange).

formulation were significant for all studied texture parameters ( $F_L$ ,  $F_T$  and AI), the interaction torque\*formulation was not significant for any of them (see Table 4), meaning that torque influenced texture regardless of the ingredients used. For all formulations, torque values were positively correlated with  $F_L$ ,  $F_T$  and AI (Fig. 5A, 5B and 5C, respectively), explaining an important part of the changes that occur in texture formation ( $R^2 = 0.77$ , 0.87 and 0.75, respectively). Higher torque values allowed the obtention of better texturised HME and, at values higher than 8 %, fibrous structures were developed in all HME ( $AI > 1$ ).

The fact that torque allows to obtain information on HME texturisation for all different studied formulations represents a step towards reducing the costly trial-and-error attempts that are often faced in this field. Although various theories concerning structuring of extruded meat analogues have been discussed (van der Sman and van der Goot, 2023), to date, HME development is still mostly based on empirical knowledge,

as texturisation is often evaluated *a posteriori*, in the final product. However, some work has been carried out to explore approaches that could allow the prediction of texturisation. Sandoval Murillo et al. (2019) proposed a thermodynamic model and used simulation, based on phase separation under the influence of temperature or velocity gradients, to qualitatively explain fibrous structuring during HMEP of meat substitutes. Högg and Rauh (2023) recently developed an approach to categorically predict the capacity of plant-based proteins to be texturised based on calorimetric methods, establishing the minimum temperature for protein texturisation. However, although these approaches are useful to explain texturisation phenomena, their possible application for inline monitoring is not straightforward. Because torque can be measured in real time during HMEP processing and has a significant effect on the final HME texture, inline control of texturisation could be possible up to an extent only using this parameter.

Therefore, measurement of extrusion outputs can be a simple and more attainable alternative to the existing approaches, even when no significant temperature or speed changes are observed during HMEP. Further investigation of additional non-invasive technologies (e.g., infrared spectroscopy to measure moisture content in real time), combined with monitorisation of torque, could be valuable to provide a more accurate in-line control of HMEP. This could help solve process stability issues such as not well-controlled liquid and solid feed rates, facilitating appropriate adjustments during the HMEP process and preventing the obtention of undesired products, thereby reducing potential waste of material and other resources.

### 3.5. Visual evaluation of HME texture

Fig. 6 shows images of the V-shape on the longitudinal fold of HME samples and the elliptical profile after layer separation. As no significant effect of temperature was observed on textural parameters (as mentioned in Section 3.3.), only HME samples elaborated at 145 °C are included. In general, HMEs elaborated at lower liquid feed (corresponding to an overall lower moisture content) presented a more compact aspect and more pronounced V-shape, indicating that they were more texturised than those elaborated at higher liquid feed. This agrees with Dubey et al. (2024), who evaluated visual morphological characteristics of HME and found that increased feed moisture resulted in less compact fibrous structure and decrease in structural strength.

In addition to this, fibre-like structures uniting the two resulting splits were also observed after longitudinal folding of F2 and F3 samples with 50 % liquid feed (indicated with a blue arrow in Fig. 6), as well as less neat separation of the elliptical layers (breakage of the elliptical profile can be observed). Contrarily, a clear separation between the two resulting splits can be observed in less texturised samples. This indicated that HME structure was better bound in samples containing PPI, which agrees with the instrumental results discussed above (Section 3.3) showing that addition of PPI enhanced the texturisation process. This suggests that by appropriately combining different protein-rich ingredients, it is possible to texturise a broader array of protein sources using HMEP. This approach could unlock access to more sustainable, hypoallergenic, and nutritionally diverse protein alternatives, extending beyond the commonly used sources available today. In this context, it would be valuable to continue to explore the right combination of readily available low-cost vegetables, cereals and pulses, as well as other novel protein sources, not only to improve HME texture which is one of the primary features responsible for consumer acceptance (Janifer et al., 2025), but also to bring the amino acidic profile and protein quality closer to the target animal source (Hua et al., 2023; Prabha et al., 2021; Saldanha do Carmo et al., 2023).

Moreover, samples elaborated with addition of EVOO (F4) hardly presented V-shaped profile, and the elliptical layers separated more easily, supporting the instrumental findings regarding the limited protein texturisation with addition of oil to the formulation. This is in agreement with Kendler et al. (2021), who also found that an increase in

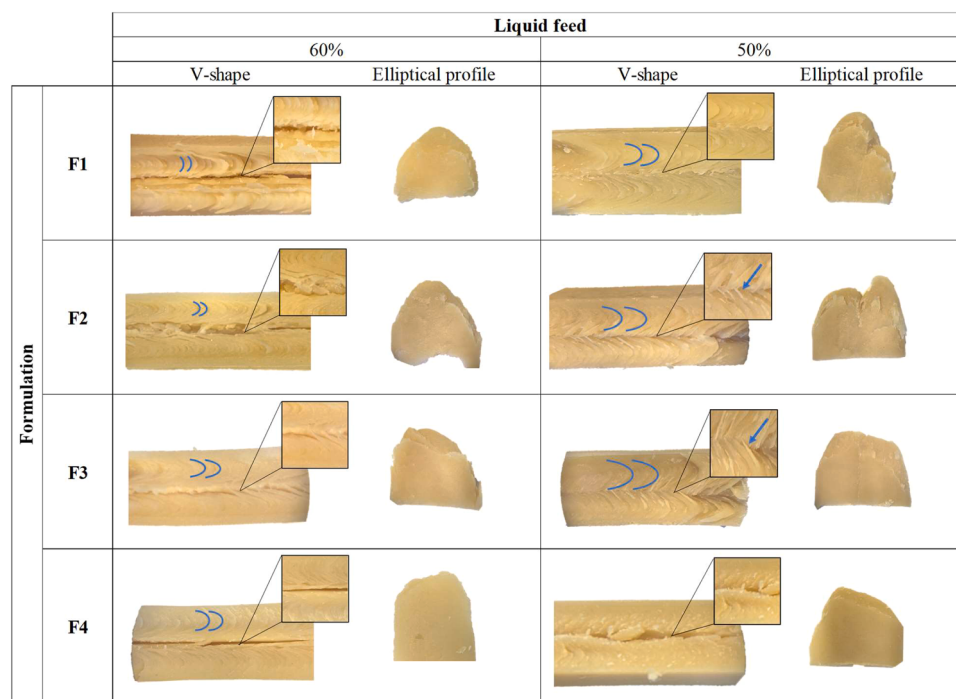


**Fig. 6.** HME V-shape (marked in blue  $\Rightarrow$ ) observed after longitudinal fold (left) and elliptical profile after layer separation (right) by formulation and liquid feed rate, for samples elaborated at 145 °C. Line between the two splits after the longitudinal fold is shown in zoomed-in images, and fibre-like structures uniting them are indicated with a blue arrow ( $\rightarrow$ ).

oil content in wheat gluten-based HME presented a more dough-like aspect and a less pronounced orientation of the flow profile (V-shape). In line with the instrumental results, this fact evidences that addition of oil during HMEP can be challenging and, although it has been demonstrated that adding it in form of emulsion with water significantly increases the amount of oil content that can be incorporated during HMEP of soy and wheat gluten blends (Wang et al., 2022), it is still an important aspect to consider during the elaboration of textured meat analogues. Given the interest in incorporating fat ingredients into HME to enhance sensory properties (Wang et al., 2022) and more effectively mimic meat in terms of nutritional profile, different methods that do not interfere with texturisation should be studied. A possible alternative would be to add oil after HMEP in posterior stages, such as a marinating process, which would allow its incorporation once the fibre-like texture of the HME has already been formed.

Although V-shape profile was slightly present in samples elaborated

at 60 % liquid feed, instrumental AI did not detect fibrousness in the direction of the extrusion flow in samples with highest moisture content. Still, in general, the visual aspect of the samples correlated with the measured AI (samples with more fibrous aspect present higher values of AI), suggesting that instrumental measure of AI can be a useful tool to evaluate HME texturisation in samples with less moisture content.

### 3.6. Microstructure of highly texturised HME

As HME produced with FBPC-PPI blends showed better texturisation, a sample produced using F3 with 50 % water feed and at 145 °C was selected as an example of highly texturised HME to be studied at a microstructural level. Fig. 7 shows a CLSM image (Fig. 7A) and a SEM image (Fig. 7B) of the selected sample.

In the CLSM image, red areas indicated presence of protein, which strongly binds with Rhodamine B. In this regard, several HMEP-related

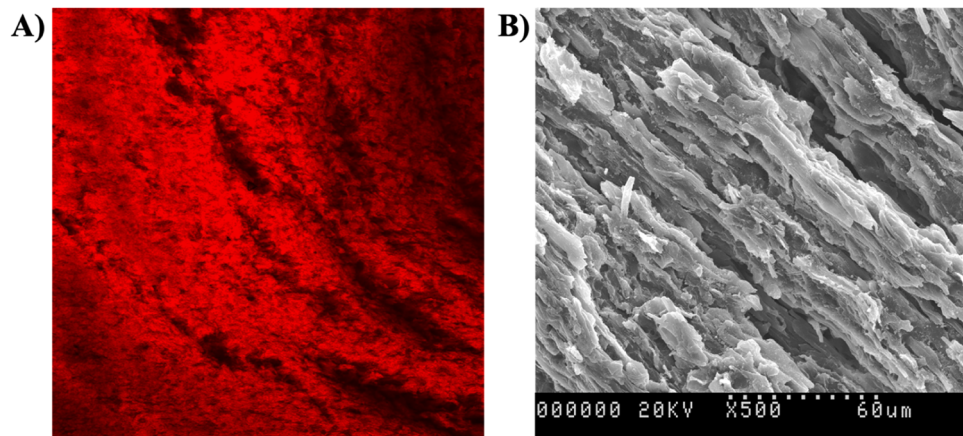


**Fig. 7.** CLSM image of FBPC-PPI (50 FBPC:50 PPI) HME produced with 50 % water feed at 145 °C, sliced and stained with Rhodamine B (A), and SEM image at magnification 500X (B).

studies have shown that difference in red intensity can be related to areas that have absorbed less water and have therefore more protein concentration (more intense red) and areas with less protein content (less intense red) (Dekkers et al., 2018). Different intensities of red colour can be observed in Fig. 7A, suggesting that texturised FBPC-PPI HME contained areas with different protein content. This could be related to the hypothesis that fibrous structures are built by protein-rich and water-rich domains (Sandoval Murillo et al., 2019). Other works have also related differences of red colour intensity in CLSM images with different affinity of the ingredients used with Rhodamine B. For example, Schreuders, Dekkers, et al. (2019) suggested that wheat gluten attained a higher intensity of the red than PPI due to its stronger affinity of Rhodamine B and its higher local concentration due to its lower water binding relative to PPI. Similarly, different red shades in Fig. 7A could also be indicating areas where the different ingredients used – in this case PPI or FBPC – are differently distributed along the sample, as they might bind differently with water, resulting in more (or less) protein-concentrated areas.

As for the SEM image (Fig. 7B), it clearly shows how the selected HME sample matrix was organised in dense, layered structures, that could be part of the larger fibres visually observed (shown in Fig. 6). This could potentially be related to the protein crosslinking and reorganization occurring during HMEP, which results in dense matrices (Peng et al., 2022) that are then aligned in the cooling stage. At the same time, the high solids content increases viscosity, allowing for greater compression of the melt during solidification, resulting in a more defined fibrous structure (Zhang, Zhang, et al., 2023). Moreover, in the work of Fan et al. (2025), SEM images of chicken meat showed similar dense, layered fibrous structures. This suggests that FBPC-PPI blends can not only show anisotropic character from instrumental texture parameters or visual observation, but also form dense, layered, fibre-like structures at a microstructural level that resemble real chicken meat.

#### 4. Conclusions

Formulation (protein source and added oil) and moisture content had a significant effect on textural characteristics of HME from FBPC, while a variation of barrel temperature of 10 °C (from 145 to 155 °C) was not sufficient to influence the final product texture. Addition of PPI increased hardness and fibrousness of the product, suggesting that the appropriate combination of different protein sources could provide textural benefits and the use of a wider variety of alternative protein sources. Oil addition had a lubricating effect which difficulted the formation of fibre-like structures in the direction of the extrusion flow, indicating that alternative methods for addition of oil or other types of fat that do not interfere with texturisation should continue to be studied. Moreover, results have shown that real-time torque measurements highly explain HME texturization when mass flow rate and screw speed are kept constant. This suggests that further investigation of HME texturization with variation of additional variables during the process could be carried out by assessing SME, and could eventually help reduce the reliance on resource-intensive trial-and-error methodologies. Moreover, the use of other non-invasive inline measurements in combination with torque (or SME) could be explored to provide a more accurate inline control tool to optimize HMEP in real time.

#### Ethics in publishing statement

All authors agree that:

This research presents an accurate account of the work performed, all data presented are accurate and methodologies detailed enough to permit others to replicate the work.

This manuscript represents entirely original works and/or if work and/or words of others have been used, that this has been appropriately cited or quoted and permission has been obtained where necessary.

This material has not been published in whole or in part elsewhere.

The manuscript is not currently being considered for publication in another journal.

That generative AI and AI-assisted technologies have not been utilized in the writing process or if used, disclosed in the manuscript the use of AI and AI-assisted technologies and a statement will appear in the published work.

That generative AI and AI-assisted technologies have not been used to create or alter images unless specifically used as part of the research design where such use must be described in a reproducible manner in the methods section.

All authors have been personally and actively involved in substantive work leading to the manuscript and will hold themselves jointly and individually responsible for its content.

#### CRediT authorship contribution statement

**Clara Barnés-Calle:** Writing – original draft, Methodology, Investigation, Formal analysis. **Grau Matas:** Writing – review & editing, Investigation, Formal analysis. **Pere Gou:** Writing – review & editing, Supervision, Project administration, Methodology, Investigation, Formal analysis, Conceptualization. **Elena Fulladosa:** Writing – review & editing, Supervision, Project administration, Methodology, Investigation, Formal analysis, Conceptualization.

#### Declaration of competing interest

The authors declare that they have no known competing financial interests or personal relationships that could have appeared to influence the work reported in this paper.

#### Acknowledgements

This work was financially supported by the Horizon 2020 UE programme through the project “CROPDIVA” [grant number 101000847]; by the Spanish MCIN/AEI/10.13039/501100011033/ FEDER [grant number PID2021-122285OR-I00]. Acknowledgements are extended to the Spanish MCIN/AEI/10.13039/501100011033 and FSE *invierte en tu futuro* for financing the first author’s doctorate studies [grant number FPU20/04009], to the consolidated Research Group (2021 SGR 00461) and CERCA program from Generalitat de Catalunya. The authors also want to acknowledge Clàudia Sánchez-Martínez for her contribution by performing experimental work.

#### Data availability

Data will be made available on request.

#### References

- Abeykoon, C., McAfee, M., Thompson, S., Li, K., Kelly, A.L., Brown, E.C., 2009. Investigation of Torque Fluctuations in Extrusion Through Monitoring of Motor Variables. *host publication*.
- Aiken, W., Alfrey, T., Janssen, A., Mark, H., 1947. Creep behavior of plasticized vinylite VYNW. *J. Polym. Sci.* 2 (2), 178–198. <https://doi.org/10.1002/pol.1947.120020206>.
- Akdogan, H., 1996. Pressure, torque, and energy responses of a twin screw extruder at high moisture contents. *Food Res. Int.* 29 (5–6), 423–429. [https://doi.org/10.1016/S0963-9969\(96\)00036-1](https://doi.org/10.1016/S0963-9969(96)00036-1).
- Akdogan, H., 1999. High moisture food extrusion. *Int J Food Sci Technol* 34 (3), 195–207. <https://doi.org/10.1046/j.1365-2621.1999.00256.x>.
- Alee, M., Duan, Q., Chen, Y., Liu, H., Ali, A., Zhu, J., Jiang, T., Rahaman, A., Chen, L., Yu, L., 2021. Plasticization efficiency and characteristics of monosaccharides, disaccharides, and low-molecular-weight polysaccharides for starch-based materials. *ACS Sustain. Chem. Eng.* 9 (35), 11960–11969. <https://doi.org/10.1021/acssuschemeng.1c04374>.
- Ali, S., Singh, B., Sharma, S., 2020. Effect of processing temperature on morphology, crystallinity, functional properties, and in vitro digestibility of extruded corn and potato starches. *J Food Process Preserv* 44 (7). <https://doi.org/10.1111/jfpp.14531>.
- Barnés-Calle, C., Matas, G., Claret, A., Guerrero, L., Fulladosa, E., Gou, P., 2024. High moisture extrusion of pea protein isolate to mimic chicken texture: instrumental and

- sensory insights. *Food Hydrocoll* 154, 110129. <https://doi.org/10.1016/j.foodhyd.2024.110129>.
- Bekaert, B., Van Snick, B., Pandelaere, K., Dhondt, J., Di Pretoro, G., De Beer, T., Vervaet, C., Vanhoorne, V., 2022. In-depth analysis of the long-term processability of materials during continuous feeding. *Int J Pharm* 614, 121454. <https://doi.org/10.1016/j.ijpharm.2022.121454>.
- Chandran, A.S., Kashyap, P., Thakur, M., 2024. Effect of extraction methods on functional properties of plant proteins: a review. *EFood* 5 (3). <https://doi.org/10.1002/efd2.151>.
- Chen, F.L., Wei, Y.M., Zhang, B., Ojokoh, A.O., 2010. System parameters and product properties response of soybean protein extruded at wide moisture range. *J Food Eng* 96 (2), 208–213. <https://doi.org/10.1016/j.jfoodeng.2009.07.014>.
- Chen, Q., Zhang, J., Zhang, Y., Wang, Q., 2022. Effect of fatty acid saturation degree on the rheological properties of pea protein and its high-moisture extruded product quality. *Food Chem* 390, 133139. <https://doi.org/10.1016/j.foodchem.2022.133139>.
- Chiang, J.H., Loveday, S.M., Hardacre, A.K., Parker, M.E., 2019. Effects of soy protein to wheat gluten ratio on the physicochemical properties of extruded meat analogues. *Food Struct.* 19, 100102.
- Cotacallapa-Sucapuca, M., Vega, E.N., Maieves, H.A., Berrios, J.D.J., Morales, P., Fernández-Ruiz, V., Cámaras, M., 2021. Extrusion process as an alternative to improve pulses products consumption. A review. *Foods* 10 (5), 1096. <https://doi.org/10.3390/foods10051096>.
- Dekkers, B.L., Emin, M.A., Boom, R.M., van der Goot, A.J., 2018. The phase properties of soy protein and wheat gluten in a blend for fibrous structure formation. *Food Hydrocoll* 79, 273–281. <https://doi.org/10.1016/j.foodhyd.2017.12.033>.
- Dubey, A., Mateen, A., Singh, N., 2024. Exploring textural, solubility and rheological characteristics of high-moisture extruded meat analogues: effects of wheat gluten and rice protein incorporation in pea protein isolate and feed moisture levels. *Int J Food Sci Technol* 59 (8), 5560–5575. <https://doi.org/10.1111/ijfs.17279>.
- Elshamy, A.F., Rosentrater, K.A., Ghnimi, S., Hossain, M.K., Lammers, V., Heinz, V., Diakité, M., 2025. High-moisture meat analogs produced from dry-fractionated Faba bean, yellow pea, and functional soy proteins: Effects of mixture design and extrusion parameters on texture properties. *Innov. Food Sci. Emerg. Technol.* 100, 103927. [doi:10.1016/j.ifset.2025.103927](https://doi.org/10.1016/j.ifset.2025.103927).
- Fan, Y., Annamalai, P.K., Bhandari, B., Prakash, S., 2025. Characteristics of faba bean protein-based high-moisture meat analogues incorporating brewers' spent grain through extrusion. *Innov. Food Sci. Emerg. Technol.* 100, 103919. <https://doi.org/10.1016/j.ifset.2025.103919>.
- Ferawati, F., Zahari, I., Barman, M., Ahlström, C., Witthöft, C., Östbring, K., 2021. High-moisture meat analogues produced from yellow pea and faba bean protein isolates/concentrate: effect of raw material composition and extrusion parameters on texture properties. *Foods* 10 (4). <https://doi.org/10.3390/foods10040843>.
- Gao, W., Liu, P., Li, X., Qiu, L., Hou, H., Cui, B., 2019. The co-plasticization effects of glycerol and small molecular sugars on starch-based nanocomposite films prepared by extrusion blowing. *Int. J. Biol. Macromol* 133, 1175–1181. <https://doi.org/10.1016/j.ijbiomac.2019.04.193>.
- Godavarti, S., Karwe, M., 1997. Determination of specific mechanical energy distribution on a twin-screw extruder. *J. Agric. Eng. Res.* 67 (4), 277–287. <https://doi.org/10.1006/jaer.1997.0172>.
- Guerrero, P., Beatty, E., Kerry, J.P., de la Caba, K., 2012. Extrusion of soy protein with gelatin and sugars at low moisture content. *J Food Eng* 110 (1), 53–59. <https://doi.org/10.1016/j.jfoodeng.2011.12.009>.
- Gwiazda, S., Noguchi, A., Saio, K., 1987. Microstructural studies of texturised vegetable protein products: effects of oil addition and transformation of raw materials in various sections of a twin screw extruder. *Food Struct.* 6 (1).
- Hao, S., Zheng, Y., Li, M., Feng, X., Yang, X., 2024. Effects of heat-moisture extrusion on the structure and functional properties of protein-fortified whole potato flour. *Food Chem.* X 24, 102048. <https://doi.org/10.1016/j.fochx.2024.102048>.
- Högg, E., Rauh, C., 2023. Towards a better understanding of texturisation during high-moisture extrusion (HME)—Part I: modeling the texturability of plant-based proteins. *Foods* 12 (10), 1955. <https://doi.org/10.3390/foods12101955>.
- Hopf, A., Dehghani, F., Buckow, R., 2023. Dry fractionation of plant-based proteins for better meat analogue applications. *Curr. Food Sci. Technol. Rep.* 1 (2), 91–98. <https://doi.org/10.1007/s43555-023-00009-1>.
- Hua, X.Y., Long, Y., Ong, D.S.M., Theng, A.H.P., Shi, J.K., Osen, R., Wu, M., Chiang, J.H., 2023. Mathematical optimisation of extruded mixed plant protein-based meat analogues based on amino acid compositions. *Curr. Res. Food Sci.* 7, 100648. <https://doi.org/10.1016/j.crfc.2023.100648>.
- Ilo, S., Schoenlechner, R., Bergthofe, E., 2000. Role of lipids in the extrusion cooking processes. *Grasas Aceites* 51 (1–2). <https://doi.org/10.3989/gya.2000.v51.i1-2.410>.
- Immonen, M., Chandrakusuma, A., Sibakov, J., Poikelispää, M., Sontag-Strohm, T., 2021. Texturisation of a blend of pea and de starched oat protein using high-moisture extrusion. *Foods* 10 (7), 1517. <https://doi.org/10.3390/foods10071517>.
- Janifer, R.X., Sahana, H.S., Dimple, V., Om, P.C., 2025. Future trends in plant-based meat: consumer perception, market growth and health benefits. *Future Foods*, 100551. <https://doi.org/10.1016/j.fufo.2025.100551>. ISSN 2666-8335.
- Kantanen, K., Oksanen, A., Edelmann, M., Suhonen, H., Sontag-Strohm, T., Piironen, V., Ramos Diaz, J.M., Jouppila, K., 2022. Physical properties of extrudates with fibrous structures made of Faba Bean protein ingredients using high moisture extrusion. *Foods* 11 (9), 1280. <https://doi.org/10.3390/foods11091280>.
- Kantrong, H., Charunuch, C., Limsangouan, N., Pengpinit, W., 2018. Influence of process parameters on physical properties and specific mechanical energy of healthy mushroom-rice snacks and optimization of extrusion process parameters using response surface methodology. *J Food Sci Technol* 55 (9), 3462–3472. <https://doi.org/10.1007/s13197-018-3271-2>.
- Kendler, C., Duchardt, A., Karbstein, H.P., Emin, M.A., 2021. Effect of oil content and oil addition point on the extrusion processing of wheat gluten-based meat analogues. *Foods* 10 (4), 697. <https://doi.org/10.3390/foods10040697>.
- Mennig, G., 1987. The torque in the metering zone of single screw extruders. *Polym. Eng. Sci.* 27 (3), 181–185. <https://doi.org/10.1002/pen.760270302>.
- Oluwajuyitan, T.D., Aluko, R.E., 2025. Structural and functional properties of fava bean albumin, globulin and glutelin protein fractions. *Food Chem.* X 25, 102104. <https://doi.org/10.1016/j.fochx.2024.102104>.
- Opaluwa, C., Deskovski, S., Karbstein, H.P., Emin, M.A., 2024. Effect of oil on the rheological properties and reaction behavior of highly concentrated wheat gluten under conditions relevant to high moisture extrusion. *Future Foods* 9, 100307. <https://doi.org/10.1016/j.fufo.2024.100307>.
- Osen, R., Toelstede, S., Wild, F., Eisner, P., Schweiggert-Weisz, U., 2014. High moisture extrusion cooking of pea protein isolates: raw material characteristics, extruder responses, and texture properties. *J Food Eng* 127, 67–74. <https://doi.org/10.1016/j.jfoodeng.2013.11.023>.
- Osborne, T.B., 1924. *The vegetable proteins*. Longmans, Green and Company.
- Osen, R., 2017. Texturisation of Pea Protein Isolates Using High Moisture Extrusion Cooking. Technische Universität München. <https://nbn-resolving.de/urn/resolver.pl?urn=nbn:de:bvb:91-diss-20171009-1356359-1-4>.
- Peng, H., Zhang, J., Wang, S., Qi, M., Yue, M., Zhang, S., Song, J., Wang, C., Zhang, D., Wang, X., Ma, C., 2022. High moisture extrusion of pea protein: effect of L-cysteine on product properties and the process forming a fibrous structure. *Food Hydrocoll* 129, 107633. <https://doi.org/10.1016/j.foodhyd.2022.107633>.
- Pietsch, V.L., Bühl, J.M., Karbstein, H.P., Emin, M.A., 2019. High moisture extrusion of soy protein concentrate: influence of thermomechanical treatment on protein-protein interactions and rheological properties. *J Food Eng* 251, 11–18. <https://doi.org/10.1016/j.jfoodeng.2019.01.001>.
- Plattner, B., 2020. Extrusion Techniques for Meat Analogues. *Cereal Foods World* 65 (4). [doi:10.1094/CFW-65-4-0043](https://doi.org/10.1094/CFW-65-4-0043).
- Prabha, K., Ghosh, P., Abdulla, S., Joseph, R.M., Krishnan, R., Rana, S.S., Pradhan, R.C., 2021. Recent development, challenges, and prospects of extrusion technology. *Future Foods* 3, 100019. <https://doi.org/10.1016/j.fufo.2021.100019>.
- Ranasinghesagara, J., Hsieh, F., Yao, G., 2005. An Image Processing Method for Quantifying Fiber Formation in Meat Analogs Under High Moisture Extrusion. *J. Food Sci.* 70 (8). [doi:10.1111/j.1365-2621.2005.tb11513.x](https://doi.org/10.1111/j.1365-2621.2005.tb11513.x).
- Ribeiro, G., Piñero, M.-Y., Parle, F., Blanco, B., Roman, L., 2024. Optimizing screw speed and barrel temperature for textural and nutritional improvement of soy-based high-moisture extrudates. *Foods* 13 (11), 1748. <https://doi.org/10.3390/foods13111748>.
- Saavedra Isusi, G.I., Pietsch, V., Beutler, P., Hoehne, S., Leister, N., 2023. Influence of rapeseed oil on extruded plant-based meat analogues: assessing mechanical and rheological properties. *Processes* 11, 1871. <https://doi.org/10.3390/pr11071871>.
- Saldanha do Carmo, C., Knutsen, S.H., Malizia, G., Dessev, T., Geny, A., Zobel, H., Myhrer, K.S., Varela, P., Sahlstrom, S., 2021. Meat analogues from a faba bean concentrate can be generated by high moisture extrusion. *Future Foods* 3, 100014. <https://doi.org/10.1016/j.fufo.2021.100014>. ISSN 2666-8335.
- Saldanha do Carmo, C., Rieder, A., Varela, P., Zobel, H., Dessev, T., Nersten, S., Gaber, S., M., Sahlstrom, S., Knutsen, S.H., 2023. Texturized vegetable protein from a faba bean protein concentrate and an oat fraction: impact on physicochemical, nutritional, textural and sensory properties. *Future Foods* 7, 100228. <https://doi.org/10.1016/j.fufo.2023.100228>. ISSN 2666-8335.
- Samard, S., Gu, B.Y., Ryu, G.H., 2019. Effects of extrusion types, screw speed and addition of wheat gluten on physicochemical characteristics and cooking stability of meat analogues. *J. Sci. Food Agric* 99 (11), 4922–4931. <https://doi.org/10.1002/jsfa.9722>.
- Sandoval Murillo, J.L., Osen, R., Hiermaier, S., Ganzenmüller, G., 2019. Towards understanding the mechanism of fibrous texture formation during high-moisture extrusion of meat substitutes. *J Food Eng* 242, 8–20. <https://doi.org/10.1016/j.jfoodeng.2018.08.009>.
- Schmid, E., Farahanyk, A., Adhikari, B., Torley, P.J., 2022. High moisture extrusion cooking of meat analogs: a review of mechanisms of protein texturisation. *Compr. Rev. Food Sci. Food Saf.* 21 (6), 4573–4609. <https://doi.org/10.1111/1541-4337.13030>.
- Schreuders, F.K.G., Dekkers, B.L., Bodnár, I., Erni, P., Boom, R.M., van der Goot, A.J., 2019. Comparing structuring potential of pea and soy protein with gluten for meat analogue preparation. *J Food Eng* 261, 32–39. <https://doi.org/10.1016/j.jfoodeng.2019.04.022>.
- Schreuders, F.K.G., Schlangen, M., Kyriakopoulou, K., Boom, R.M., van der Goot, A.J., 2021. Texture methods for evaluating meat and meat analogue structures: a review. *Food Control* 127, 108103. <https://doi.org/10.1016/j.foodcont.2021.108103>.
- Singh, R., Guerrero, M., Nickerson, M.T., Koksel, F., 2024. Effects of extrusion screw speed, feed moisture content, and barrel temperature on the physical, technofunctional, and microstructural quality of textured lentil protein. *J. Food Sci.* 89 (4), 2040–2053. [doi:10.1111/1750-3841.16991](https://doi.org/10.1111/1750-3841.16991).
- Soeda, T., 1994. Studies on gelation of soy protein during cold storage, 2: Effect of heating on the molecular structure of soy protein. *J. Jpn. Soc. Food Sci. Technol.* 41 (10), 676–681.
- Sun, D., Zhang, B., Zhou, C., Ren, W., Wu, M., 2023. Effect of high-moisture extrusion process on quality attribute and fibrous formation mechanism of pea protein: insight into dynamic changes of textual protein. *Innov. Food Sci. Emerg. Technol.* 89, 103486. <https://doi.org/10.1016/j.ifset.2023.103486>.
- Toldrà, M., Parés, D., Barnés-Calle, C., Gou, P., Fulladosa, E., 2025. Techno-functional and physico-chemical properties of high moisture extrudates from faba bean (*Vicia*

- faba) protein concentrate using different extrusion conditions. *LWT*, 117898. <https://doi.org/10.1016/j.lwt.2025.117898>.
- Tsagareishvili, D., Sesikashvili, O., Dadunashvili, G., Sakhanberidze, N., Tsagareishvili, S., 2019. The influence of the moisture content of raw materials on the structuring of the extrudates. *Potravin. Slovak J. Food Sci.* 13 (1), 898–905. <https://doi.org/10.5219/1189>.
- U.S Department of Agriculture (USDA), 2019. FoodData Central - chicken, broilers or fryers, breast, meat only, cooked, roasted. SR Legacy, 171477. <https://fdc.nal.usda.gov/food-details/171477/nutrients>. Accessed 05 June 2025.
- van der Sman, R.G.M., van der Goot, A.J., 2023. Hypotheses concerning structuring of extruded meat analogs. *Curr. Res. Food Sci.* 6, 100510. <https://doi.org/10.1016/j.crefs.2023.100510>.
- Verfaillie, D., Li, J., Janssen, F., Blonckrock, E., Van Royen, G., Wouters, A.G.B., 2024. Relating the protein denaturation degree and solubility of soy protein isolates to the structure of high moisture extrudates. *Food Hydrocoll* 155, 110211. <https://doi.org/10.1016/j.foodhyd.2024.110211>.
- Wagner, L.L., Baird, D.G., Wilkes, G.L., Reddy, J.N., Conger, W.L., Bevan, D.R., 1987. Numerical Modeling of the Cooking Extrusion of a Bio-Polymer. Virginia Polytechnic Institute and State University [Dissertation]. <http://hdl.handle.net/10919/53662>.
- Wang, H., Zhang, L., Czaja, T.P., Bakalis, S., Zhang, W., Lametsch, R., 2022. Structural characteristics of high-moisture extrudates with oil-in-water emulsions. *Food Res. Int.* 158, 111554. <https://doi.org/10.1016/j.foodres.2022.111554>.
- Wittek, P., Karbstein, H.P., Emin, M.A., 2021. Blending proteins in high moisture extrusion to design meat analogues: rheological properties, morphology development and product properties. *Foods* 10 (7), 1509. <https://doi.org/10.3390/foods10071509>.
- Wittek, P., Zeiler, N., Karbstein, H.P., Emin, M.A., 2021. High moisture extrusion of soy protein: investigations on the formation of anisotropic product structure. *Foods* 10 (1), 102. <https://doi.org/10.3390/foods10010102>.
- Wolz, M., Kulozik, U., 2017. System parameters in a high moisture extrusion process for microparticulation of whey proteins. *J Food Eng* 209, 12–17. <https://doi.org/10.1016/j.jfoodeng.2017.04.010>.
- Xia, S., Song, J., Ma, C., Hao, T., Hou, Y., Shen, S., Li, K., Ma, L., Xue, Y., Xue, C., Jiang, X., 2023. Effects of moisture content and processing temperature on the strength and orientation regulation of fibrous structures in meat analogues. *Food Hydrocoll* 145, 109113. <https://doi.org/10.1016/j.foodhyd.2023.109113>.
- Yao, G., Liu, K.S., Hsieh, F., 2004. A new method for characterizing Fiber formation in meat analogs during high-moisture extrusion. *J. Food Sci* 69 (7), 303–307. <https://doi.org/10.1111/j.1365-2621.2004.tb13634.x>.
- Zang, Y., Yang, R., Wang, S., Sun, C., Zhao, Y., Cao, Y., Lu, W., Zhang, Y., Fang, Y., 2025. High-moisture soy protein extrudates with different moisture contents: texture, structure, and in vitro digestion characteristics. *Food Res. Int.* 210, 116412. <https://doi.org/10.1016/j.foodres.2025.116412>.
- Zhang, J., Liu, L., Zhu, S., Wang, Q., 2018. Texturisation behaviour of peanut–soy bean/wheat protein mixtures during high moisture extrusion cooking. *Int J Food Sci Technol* 53 (11), 2535–2541. <https://doi.org/10.1111/ijfs.13847>.
- Zhang, X., Zhao, Y., Zhao, X., Sun, P., Zhao, D., Jiang, L., Sui, X., 2023. The texture of plant protein-based meat analogs by high moisture extrusion: a review. *J Texture Stud* 54 (3), 351–364. <https://doi.org/10.1111/jtxs.12697>.
- Zhang, Z., Zhang, L., He, S., Li, X., Jin, R., Liu, Q., Chen, S., Sun, H., 2023. High-moisture extrusion technology application in the processing of textured plant protein meat analogues: a review. *Food Rev. Int.* 39 (8), 4873–4908. <https://doi.org/10.1080/87559129.2021.2024223>.
- Zhao, Z., Wang, Z., He, Z., Zeng, M., Chen, J., 2023. Effects of process parameters on the fibrous structure and textural properties of calcium caseinate extrudates. *Polym. (Basel)* 15 (5), 1292. <https://doi.org/10.3390/polym15051292>.